A crossed molecular beam and *ab initio* investigation of the exclusive methyl loss pathway in the gas phase reaction of boron monoxide (BO; X²Σ⁺) with dimethylacetylene (CH₃CCCH₃; X¹A₁g)†

Ralf I. Kaiser,*[a] Surajit Maity,[a] Beni B. Dangi,[a] Yuan-Siang Su,[b] B. J. Sun[b] and Agnes H. H. Chang*[b]

The crossed molecular beam reaction of boron monoxide (^{11}BO; X$^2\Sigma^+$) with dimethylacetylene (CH$_3$CCCH$_3$; X^{1}A$_{1g}$) was investigated at a collision energy of 23.9 ± 1.5 kJ mol^{-1}. The scattering dynamics were suggested to be indirect (complex forming reaction) and were initiated by the addition of ^{11}BO(X$^2\Sigma^+$) with the radical center located at the boron atom to the π electron density at the acetylenic carbon–carbon triple bond without entrance barrier leading to *cis–trans* ^{11}BOC$_4$H$_6$ doublet radical intermediates. *cis*-^{11}BOC$_4$H$_6$ underwent *cis–trans* isomerization followed by unimolecular decomposition *via* a methyl group (CH$_3$) loss forming 1-propynyl boron monoxide (CH$_3$CC^{11}BO) in an overall exoergic reaction (experimental: −91 ± 22 kJ mol^{-1}; theoretical: −105 ± 9 kJ mol^{-1}; NIST: −104 ± 12 kJ mol^{-1}) *via* a tight exit transition state; *trans*-^{11}BOC$_4$H$_6$ was found to lose a methyl group instantaneously. Neither atomic nor molecular hydrogen loss pathways were detectable. The experimental finding of an exclusive methyl loss pathway gains full support from our computational study predicting a methyl group *versus* atomic hydrogen loss branching ratio of 99.99% to 0.01% forming 1-propynyl boron monoxide (CH$_3$CC^{11}BO) and 1-methyl-propadienyl boron monoxide (CH$_3$(^{11}BO)CCCH$_2$), respectively.

1. Introduction

An understanding of the energetics and dynamics of elementary reactions of boron monoxide (^{11}BO; X$^2\Sigma^+$) radicals with key unsaturated hydrocarbons [acetylene (C$_2$H$_2$(X$^1\Sigma_g^+$)), ethylene (C$_2$H$_4$(X^{1}A$_g$)), methylacetylene (CH$_3$CCH(X^{1}A$_1$)), allene (H$_2$CCCH$_2$(X^{1}A$_1$)), dimethylacetylene (CH$_3$CCCH$_3$(X^{1}A$_{1g}$)), diacetylene (C$_4$H$_2$(X$^1\Sigma_g^+$)), and benzene (C$_6$H$_6$ (X^{1}A$_{1g}$))] and the inherent formation of small boron–oxygen-bearing molecules is of considerable interest to understand boron combustion processes, to the physical organic community due to the isoelectronic nature of boron monoxide and the cyano radical reactants, and to the reaction dynamics community (reaction dynamics of transient radicals) both from the experimental and theoretical viewpoints.

First, boron monoxide presents a crucial transient radical in boron-based combustion processes, but the reaction dynamics of this radical have not been investigated so far. Here, due to its

high energy density, boron has long been regarded as a good candidate for rocket fuel additives.[1–3] This feature has also been expanded recently to ramjet and scramjet propulsion systems. The oxidation of boron is initially unable to achieve full energy release due to the formation of boron oxide (B$_2$O$_3$) as an inert layer, which coats the non-reacted boron preventing further reaction.[4] Essentially, the carbon-based fuel ignites and reaches a high enough temperature to remove the boron oxide layer, which, in turn, allows clean boron to be accessible for the combustion phase. The very first boron-bearing species formed in these processes is the boron oxide radical (^{11}BO; X$^2\Sigma^+$),[4,5] which can either react with oxygen to form ultimately boron oxide (B$_2$O$_3$) or with the hydrocarbon fuel to yield carbon-, hydrogen-, oxygen-, and boron-bearing molecules (CHOB molecules). Therefore, compared to 'classical' hydrocarbon flames, the incorporation of boron results in a more complex, high temperature (1800–4000 K) organoboron chemistry. These considerations led to the development of boron-based combustion models involving detailed experimental input parameters such as reaction products, intermediates, and rate constants. Although the reaction dynamics of boron atoms with hydrocarbon molecules[6] have emerged during recent years utilizing the crossed molecular beam approach thus accessing the B–C–H system, dynamics studies on the B–O–C–H system – in particular those involving reactions of the boron monoxide

[a] *Department of Chemistry, University of Hawai'i at Manoa, Honolulu, HI 96822, USA. E-mail: ralfk@hawaii.edu*

[b] *Department of Chemistry, National Dong Hwa University, Hualien, 974, Taiwan. E-mail: hhchang@mail.ndhu.edu.tw*

† Electronic supplementary information (ESI) available. See DOI: 10.1039/c3cp53930j

This journal is © the Owner Societies 2014

Phys. Chem. Chem. Phys., 2014, **16**, 989–997 | 989

radical (^{11}BO; X$^2\Sigma^+$) with hydrocarbon molecules – have been in its infancy. Therefore, a critical shortcoming of all boron-based combustion models is the fact that elementary reactions in the B–O system have never been coupled with those occurring in the B–C–H system. A variety of models have been developed to simulate the core parts of the combustion cycle based on the rate of diffusion of oxygen and boron through the boron oxide layers. King developed an early model[7] with the diffusion rate of oxygen through the oxide layer as the rate determining step. This model was refuted by Williams and Li[8] and Kuo and Yeh[9] who proposed a model with the diffusion of boron through the oxide layer as the rate determining step based on the experiments of Kuo and Yeh. Nevertheless, the question over the dominant diffusion process has remained inconclusive. Rabitz et al.[10] investigated a molecular level gas phase kinetic model for the homogenous chemistry of the B–O–C–H combustion system. The authors acknowledged that insufficient experimental data exist to complete this model. Information like the entrance barriers, rates of reactions, and products are lacking. A recent model[11,12] derived from Kuo et al.'s approach utilized generic global reactions in three stages: particle heating without reaction (ignition delay), first stage of combustion (oxide layer removal), and second stage of combustion (clean boron oxidation). Until now, the Rabitz et al. model remains the most comprehensive and it is utilized to investigate simpler models like those of Pfitzner et al.,[11,12] highlighting the demand for experimentally determined input parameters.

Second, besides being of interest to the combustion community, the boron monoxide radical (BO; X$^2\Sigma^+$) is of interest to the physical organic community as it is isoelectronic to the cyano radical (CN; X$^2\Sigma^+$).[13–15] A computational investigation on the vertical and electron detachment energies of boronyl substituted acetylene and the corresponding cyano substitutes was conducted recently.[13] Here, the system was compared to similar cyano substituted hydrocarbons[16–18] and it was found that the boronyl group serves as a sigma-radical in these covalent systems similar to the cyano group in substituted hydrocarbons and hydrogen in hydrocarbons. Due to the isoelectronic character of the boron monoxide and the cyano radical, the reaction dynamics and potential energy surface of the reactions of boron monoxide with unsaturated hydrocarbons can be compared with those of the isoelectronic cyano radical with unsaturated hydrocarbons studied previously by our group.[19] This helps to better rationalize basic concepts of molecular structure and chemical bonding and incorporation of boron monoxide versus the cyano radical in organic molecules. Therefore, the elucidation of reaction mechanisms involving boron monoxide radicals and a comparison with the corresponding cyano-analog systems under single collision conditions can help to shed light not only on the reactivity of ground state boron monoxide versus cyano radicals, but also on the resulting molecular structures of CHOB molecules and chemical bonding in the reaction products.

Third, the reactivity of boron monoxide radicals is of importance to the reaction dynamics community. Here, supersonic radical beams of sufficiently high intensity to be utilized in crossed beam experiments are difficult to prepare. Beams of diatomic

transient radicals are particularly difficult to prepare, and only supersonic beams of methylidyne (CH; X$^2\Pi$) reacting with molecular hydrogen,[20] acetylene,[21] and ethylene,[22] hydroxyl (OH; X$^2\Pi$),[23,24] dicarbon (C$_2$, a$^3\Pi_u$),[25] and cyano radicals (CN; X$^2\Sigma^+$)[26] have been employed successfully in crossed beam experiments. With the exception of the reactions of boron monoxide with acetylene[27] and ethylene,[28] an investigation of the reaction dynamics of boron monoxide radicals (^{11}BO; X$^2\Sigma^+$) has remained mainly elusive.

Therefore, despite the importance of boron monoxide radical reactions and the inherent formation of carbon-, hydrogen-, oxygen-, and boron-bearing (CHOB) molecules, the fundamental question 'What are the nature and the underlying reaction dynamics leading to their formation?' has not been conclusively resolved. To assess the role of the reactions of boron monoxide radicals and to include them in the pertinent boron-based combustion models, four kinds of data are crucial to obtain a legitimate and realistic picture of the formation of boron-bearing molecules and their precursors. These are: (i) data on enthalpies of formation of important reaction products, (ii) detailed data on the intermediates which can be stabilized and/or undergo further reactions in a high pressure setting, (iii) the actual reaction products under single collision conditions, and (iv) basic information on the chemical reactions and their dynamics by comparing these systems with isoelectronic reactions of cyano radicals to bridge the experimental results with theoretical computations. These data are needed by modelers simulating effects of pressure, temperature, and chemical composition in ignition and combustion systems as found in gas turbines, ramjets, scramjets, pulsed detonation engines, and chemical rockets. Finally, these investigations help to elucidate reaction mechanisms and isomerization processes of organic transient species on the most fundamental, microscopic level to transfer our knowledge to the physical organic chemistry community.

Here, we expand these studies of boron monoxide reactions and investigate the reaction dynamics of boron monoxide with dimethylacetylene (CH$_3$CCCH$_3$) to elucidate the reaction dynamics of boron monoxide with unsaturated hydrocarbon molecules under single collision reaction conditions. Dimethylacetylene (CH$_3$CCCH$_3$) is the simplest member of a di-substituted (with alkyl groups) acetylene. We will also compare the reaction dynamics of the title reaction with those of the isoelectronic reaction of cyano radicals (CN; X$^2\Sigma^+$) with dimethylacetylene (CH$_3$CCCH$_3$) studied previously under single collision conditions[17] and also with the reaction of boron monoxide with acetylene (HCCH).[27]

2. Experimental and data analysis

A crossed molecular beam machine was exploited to study the reaction of the ground state boron monoxide radical (BO; X$^2\Sigma^+$) with dimethylacetylene (CH$_3$CCCH$_3$; X^{1}A$_{1g}$) under single collision conditions.[29–33] Briefly, a supersonic beam of ground state boron monoxide (BO; X$^2\Sigma^+$) was prepared in situ via laser ablation of a boron rod at 266 nm and seeding the ablated boron in pure carbon dioxide carrier gas (CO$_2$, 99.99%, BOC gases).[34] The fourth

990 | Phys. Chem. Chem. Phys., 2014, **16**, 989–997

This journal is © the Owner Societies 2014

harmonic output of a Spectra-Physic Quanta-Ray Pro 270 Nd:YAG laser (266 nm) operated at a repetition rate of 30 Hz and was focused with an output power of 15 to 20 mJ per pulse onto the rotating boron rod using a lens of 1500 mm focal length.[34] The carbon dioxide gas was released by a Proch–Trickl pulsed valve with a nozzle diameter of 1 mm driven at 60 Hz with 80 μs pulse width and −350 V pulse amplitude.[35] A backing pressure of 4 atm was used, which yielded a pressure of 5×10^{-4} Torr inside the primary source chamber. A 11.2 ± 0.1 μs segment of the beam, which passed through a skimmer of diameter 1 mm, was selected by a four-slot chopper wheel placed 18 mm downstream the skimmer; the chopper operated at a frequency of 120 Hz. The segment of the boron monoxide beam was characterized by a peak velocity (v_p) of 1426 ± 35 ms^{-1} and a speed ratio (S) of 2.2 ± 0.3. The ro-vibrational levels of this segment of the boron monoxide radical were characterized *in situ via* laser induced fluorescence (LIF) spectroscopy.[36] Here, the $^2\Sigma^+$ electronic ground state of the boron monoxide radical was probed *via* the A$^2\Pi$–X$^2\Sigma^+$ transition. The (0,0) vibrational band near 425 nm was recorded by using the Nd:YAG pumped Lambda Physik Scanmate dye laser output of about 10 μJ per pulse. The spectra were analyzed using the diatomic spectral simulation program developed by Tan.[37] The rotational temperature was determined to be 250 K.[36] This indicates that the ^{11}BO radicals have a maximum of 2 kJ mol^{-1} of internal energy.[28,36] The LIF spectrum of the ^{11}BO radical did not show any (1,1) vibrational band; based on the noise, less than 5% of the ^{11}BO radical were suggested to reside in the $v = 1$ level.[36]

This segment of the primary beam crossed a second pulsed molecular beam of dimethylacetylene perpendicularly in the interaction region. Dimethylacetylene (Aldrich; 99%+) was released by a second Proch–Trickl pulsed valve operating at a repetition rate of 60 Hz with an 80 μs pulse width from a backing pressure of 550 Torr; the crossed segment was characterized by a peak velocity of 790 ± 10 ms^{-1} and speed ratio (S) of 8.2 ± 0.4. The collision energy between ^{11}BO(X$^2\Sigma^+$) and dimethylacetylene was determined to be 23.9 ± 1.5 kJ mol^{-1}. Both pulsed valves, laser pulse and the chopper wheel were synchronized by three digital pulse generators (Stanford Research System, DG535) with the help of two frequency dividers (Pulse Research Lab, PRL-220A). The time zero trigger originates from an infrared photo diode (Newark Electronics; OPB960), mounted on the top of the chopper wheel. The primary and the secondary pulsed valves were triggered 1890 μs and 1865 μs, respectively, after the time zero trigger pulse with the secondary beam being slower than the primary beam. The laser was triggered 146 μs after the trigger pulse to the primary pulsed valve.

The reactively scattered products were monitored using a triply differentially pumped quadrupole mass spectrometer (QMS) in the time-of-flight (TOF) mode after electron-impact ionization of the neutral species at 80 eV electron energy with an emission current of 2 mA. The extracted ions pass through the quadrupole mass filter (Extrel QC 150) operated with an oscillator frequency of 2.1 MHz. Only ions with selected mass-to-charge (m/z) pass through the quadrupole mass filter and are accelerated towards a stainless still target coated with a thin

layer of aluminum maintained at a voltage of −22.5 kV. The ions hit the surface and initiate an electron cascade until it reaches an aluminum coated organic scintillator, whose photon cascade is detected by a photomultiplier tube (PMT, Burle, Model 8850) operated at −1.35 kV. The signal from the PMT was then filtered using a discriminator (Advanced Research Instruments, Model F-100TD, level: 1.6 mV) prior to feeding into a multichannel scaler (Stanford Research System SR430) to record the time of flight spectra.[31,33] The detector is rotatable in the plane defined by the primary and the secondary reactant beams to allow recording angular resolved TOF spectra.

At each angle, up to 7.2×10^5 TOF spectra were accumulated to probe the methyl loss channel. The recorded TOF spectra were then integrated and normalized to extract the product angular distribution in the laboratory frame. To gain information on the reaction dynamics, the experimental data must be transformed into the center-of-mass reference frame utilizing a forward-convolution routine.[38,39] This iterative method assumes an initial choice of angular flux distribution, $T(\theta)$, and the product translational energy distribution, $P(E_T)$ in the center-of-mass frame. Laboratory TOF spectra and the laboratory angular distribution were then calculated from the $T(\theta)$ and $P(E_T)$ functions and were averaged over a grid of Newton diagrams to account for the apparatus functions and the beam spreads in velocity and direction. Best fits were obtained by iteratively refining the adjustable parameters in the center-of-mass functions within the experimental error limits of, for instance, peak velocity, speed ratio, error bars in the laboratory angular distribution. The product flux contour map, $I(\theta,u) = P(u) \times T(\theta)$, reports the intensity of the reactively scattered products (I) as a function of the CM scattering angle (θ) and product velocity (u). This plot is called the reactive *differential cross section* and gives an *image* of the chemical reaction.

3. Theoretical

Probable reaction paths in the reaction of boron monoxide (BO(X$^2\Sigma^+$)) with dimethylacetylene (CH$_3$CCCH$_3$, X^{1}A$_{1g}$) are explored using *ab initio* electronic structure calculations. The intermediates, transition states, and dissociation products are characterized such that their optimized geometries and harmonic frequencies are obtained at the level of the hybrid density functional theory, the unrestricted B3LYP/c-pVTZ.[40,41] The energies are refined with the coupled cluster[42–45] CCSD(T)/cc-pVTZ with B3LYP/cc-pVTZ zero-point energy corrections. The barrierless formation of the initial collision complex **i1** is confirmed by intrinsic reaction coordinates calculations (IRC) at unrestricted B3LYP/cc-pVTZ level of theory along the carbon–boron bond distance. The GAUSSIAN-03 program was utilized in the electronic structure calculations.[46] Further, assuming the energy is equilibrated among the molecular degrees of freedom before the reaction occurs, and provided the energy is conserved such as in molecular beam experiments, the rate constants for the individual steps were predicted *via* RRKM theory. For a reaction $A^* \xrightarrow{k} A^{\neq} \to P$, where A^* is the energized reactant,

$A^{\neq}$ represents the transition state, and P the products, the rate constant $k(E)$ may be expressed as

$$k(E) = \frac{\sigma}{h} \frac{W^{\neq}(E - E^{\neq})}{\rho(E)} \qquad (1)$$

where σ is the symmetry factor, $W^{\neq}$ the number of states of the transition state, $E^{\neq}$ the transition state energy, and ρ the density of states of the reactant. ρ and $W^{\neq}$ are computed by the saddle-point method, molecules are treated as collections of harmonic oscillators whose harmonic frequencies are obtained by B3LYP/cc-pVTZ as described above.[47] These rate constants were also exploited to predict the branching ratios of the reaction.[47]

4. Results

4.1. Laboratory data

We attempted to monitor ions at mass to charge (m/z) from $m/z = 80$ ($C_4H_5{}^{11}BO^+$) to 75 ($C_4{}^{11}BO^+/C_4H^{10}BO^+$) at various laboratory angles, but did not see any reactive scattering signal. This indicates that the reaction of dimethylacetylene (CH_3CCCH_3; 54 amu) plus boron monoxide (^{11}BO; 27 amu) neither depicts an atomic nor molecular hydrogen elimination channel. Therefore, we can conclude that no $C_4H_5{}^{11}BO$ isomers are formed in

this reaction under single collision conditions within the detection limits of our system. We then focused our attention on monitoring the methyl loss pathway by probing ions from $m/z = 66$ ($C_3H_3{}^{11}BO^+$) to $m/z = 63$ ($C_3{}^{11}BO^+/(C_3H^{10}BO^+)$). Here, the reactive scattering signal was observed from $m/z = 66$ to 63. After scaling, the TOF spectra at these mass-to-charge ratios depicted identical profiles indicating that ions from $m/z = 65$ to 63 originated from the dissociative ionization of the $^{11}BOC_3H_3$ parent (66 amu) in the electron impact ionizer of the detector. Subsequent data were taken at the mass-to-charge ratio with the best signal-to-noise, *i.e.* $m/z = 66$ (Fig. 1). Therefore, we can conclude that in the reaction of $^{11}BO(X^2\Sigma^+)$ with dimethylacetylene (CH_3CCCH_3, X^1A_{1g}), the boron monoxide *versus* methyl group loss channel leading to the formation of the $^{11}BOC_3H_3$ isomer(s) is open. In summary, the laboratory data alone suggest an exclusive methyl loss elimination pathway in the reaction of boron monoxide with dimethylacetylene and the formation of $^{11}BOC_3H_3$ isomer(s). Note that the best fits of the TOF spectra (Fig. 1) and of the laboratory angular distribution (Fig. 2) were carried out with a single channel fit and a product mass combination of 66 amu ($^{11}BOC_3H_3$) and 15 amu (CH_3). Here, the laboratory angular distribution was obtained by integrating the TOF spectra taken for the $^{11}BOC_3H_3$ product at $m/z = 66$. As expected from the kinematics of the methyl
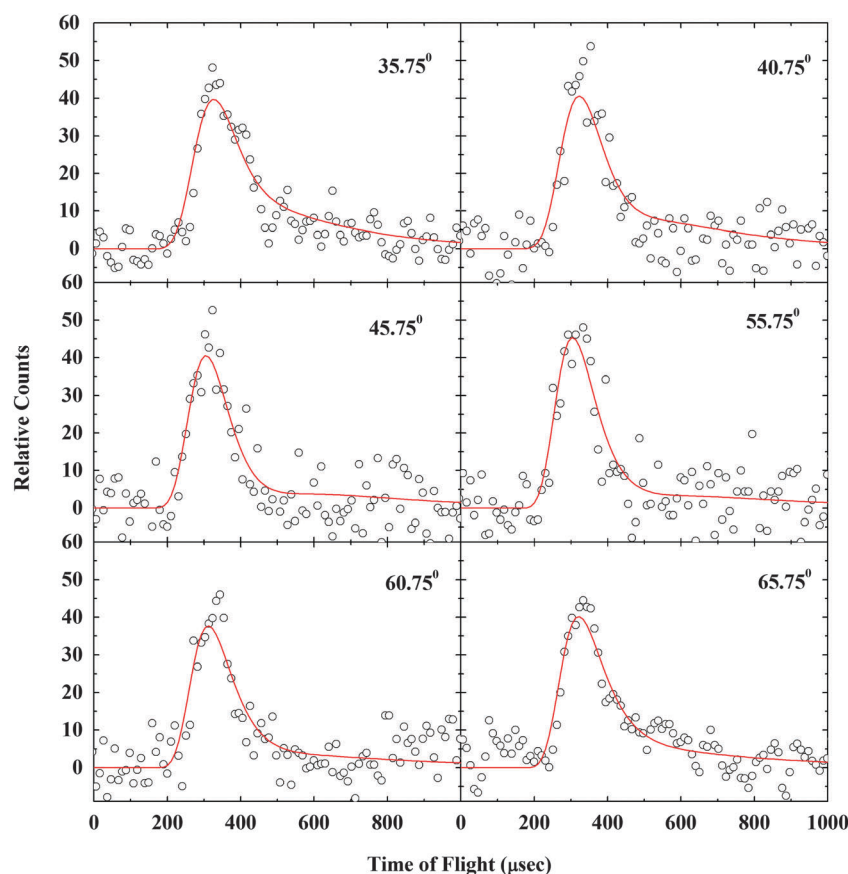

Fig. 1 Time-of-flight data recorded at $m/z = 66$ ($C_3H_3{}^{11}BO^+$) at various laboratory angles for the reaction between boron monoxide (^{11}BO; $X^2\Sigma^+$) with dimethylacetylene (CH_3CCCH_3; X^1A_{1g}) at a collision energy of 23.9 ± 1.5 kJ mol^{-1}. The circles indicate the experimental data, and the solid lines indicate the calculated fit.
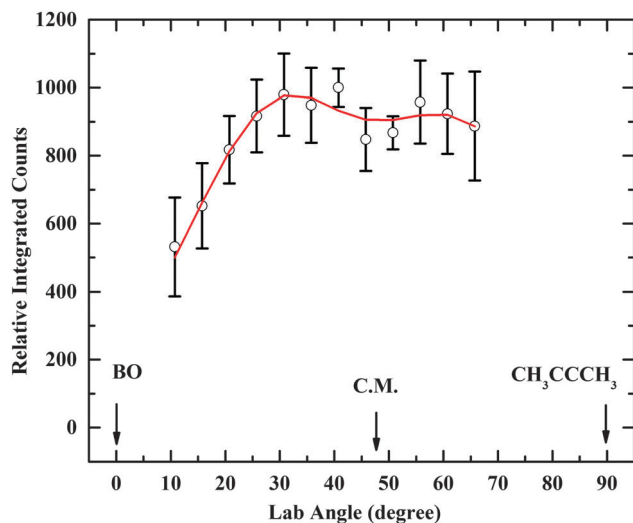
Fig. 2 Laboratory angular distribution (LAB) of ions of m/z = 66 ($C_3H_3{}^{11}BO^+$) for the reaction of boron monoxide (^{11}BO; $X^2\Sigma^+$) with dimethylacetylene (CH_3CCCH_3; X^1A_{1g}) at a collision energy of 23.9 ± 1.5 kJ mol^{-1}. The circles and error bars indicate the experimental data, and the solid line indicates the calculated distribution.

group loss channel, the angular distribution is very broad and extends over the complete detector range to at least 55.0° in the scattering plane defined by the primary and the secondary molecular beams. The laboratory angular distribution depicts a slight dip at the center of mass angle of 47.4 ± 1.0°.

4.2. Center-of-mass functions

To obtain information on the underlying reaction dynamics, we transform the data from the laboratory to the center-of-mass reference frame utilizing the forward convolution routine as described in Section 2. This leads to the center-of-mass translational ($P(E_T)$) and angular distributions ($T(\theta)$) (Fig. 3). Here, the center-of-mass translational energy distribution, $P(E_T)$, of the methyl loss channel shows a maximum translational energy (E_{max}) release of 115 ± 20 kJ mol^{-1}. For those molecules formed without internal excitation, from the conservation of energy, we can calculate the reaction exoergicity by subtracting the collision energy (23.9 ± 1.5 kJ mol^{-1}) from E_{max}. Here, we see that the reaction forming the $C_3H_3{}^{11}BO$ isomer(s) plus methyl (CH_3) is exoergic by 91 ± 22 kJ mol^{-1}. Also, as can be seen from the $P(E_T)$, the flux distribution peaks well away from zero translational energy at about 20 to 40 kJ mol^{-1}. This finding proposes that this reaction channel involves a tight exit transition state (repulsive bond rupture with a significant electron rearrangement). Finally, the $P(E_T)$ also allows us to determine the amount of energy released into the translational degrees of freedom of the products on average to be 33 ± 3 kJ mol^{-1}. This order-of-magnitude is indicative of indirect (complex forming) scattering dynamics involving $C_4H_6{}^{11}BO$ intermediates.[48]

The center-of-mass angular distribution, $T(\theta)$, as shown in Fig. 3 (bottom) also possesses important features. Most important, the distribution depicts intensity over the whole angular range from 0° to 180°. This finding is indicative of an indirect,
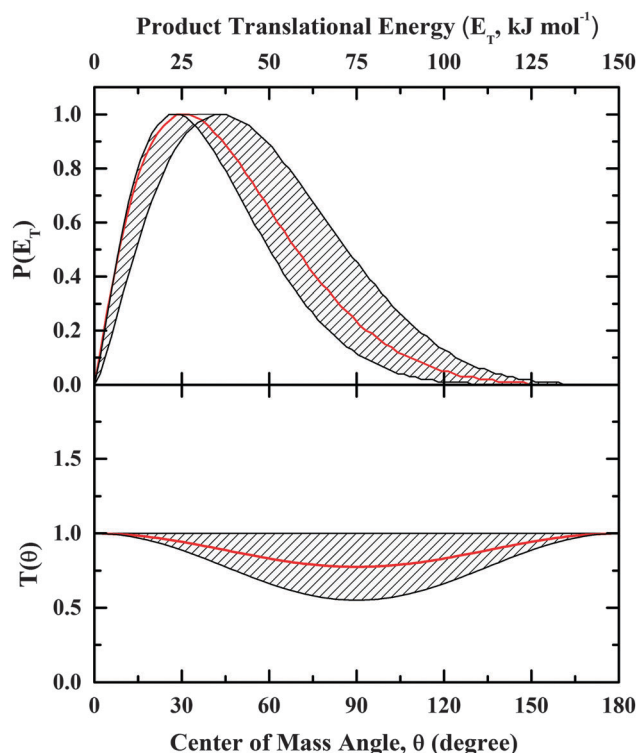

Fig. 3 Center-of-mass translational energy distribution (top) and center-of-mass angular distribution (bottom) for the methyl loss pathway leading to $C_3H_3{}^{11}BO$ isomers in the reaction of boron monoxide (^{11}BO; $X^2\Sigma^+$) with dimethylacetylene (CH_3CCCH_3; X^1A_{1g}). The hatched areas indicate the acceptable lower and upper limits of the fits and the solid red line defines the best fit functions.

complex-forming reaction mechanism involving $C_4H_6{}^{11}BO$ intermediate(s). Secondly, the center-of-mass angular distribution is forward–backward symmetric suggesting that the lifetime of the reaction intermediate is longer than its rotational period.[49] Note that in principle, the forward–backward symmetry can also be the result of a 'symmetric' reaction intermediate. In the latter case, the probability of the leaving methyl group from the decomposing complex is equal at θ and $\pi-\theta$.[49] However, none of the intermediates are symmetric (see Section 5 below) which indicates that the lifetime of the reaction intermediate is longer than its rotational period. Finally, the best fit depicts a slight distribution minimum at 90°. However, within the error limits, an isotropic (flat) distribution could fit the experimental data as well. These findings are also compiled in the flux contour maps (Fig. 4).

5. Discussion

We are merging now the experimental findings with the results of the electronic structure calculations to propose the underlying mechanism of the reaction of the boron monoxide radical with dimethylacetylene. Let us summarize the experimental results (R1–R4) first.

(R1) The boron monoxide – dimethylacetylene experiments suggest the existence of only the methyl loss pathway leading to
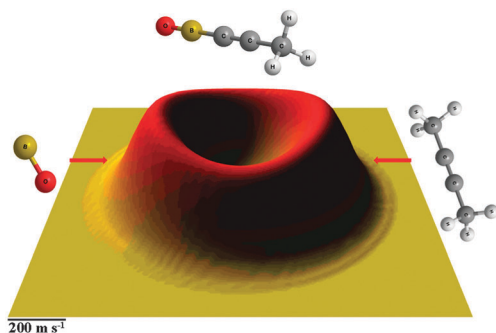
Fig. 4 The flux contour map for the methyl loss pathway leading to the 1-propynyl boron monoxide ($CH_3CC^{11}BO$) product in the reaction of boron monoxide (^{11}BO; $X^2\Sigma^+$) with dimethylacetylene (CH_3CCCH_3; X^1A_{1g}).

$^{11}BOC_3H_3$ (66 amu) and CH_3 (15 amu). Neither atomic nor molecular hydrogen loss pathways could be monitored.

(R2) The center-of-mass angular distributions of the methyl losses indicate indirect scattering dynamics *via* long-lived $^{11}BOC_4H_6$ complex(es) holding lifetimes longer than their rotation period.

(R3) The reaction energy to form $^{11}BOC_3H_3$ (66 amu) and CH_3 (15 amu) was determined to be exoergic by 91 ± 22 kJ mol^{-1} as derived from the center-of-mass translational energy distribution.

(R4) The methyl loss pathway involves a tight exit barrier in the order of 20 to 40 kJ mol^{-1}.

First, let us identify the $^{11}BOC_3H_3$ (66 amu) isomer(s) formed in the boron monoxide *versus* methyl group loss channel. Our calculations predict that this reaction pathway is overall exoergic with respect to the separated reactants by 105 ± 9 kJ mol^{-1} to form the 1-propynyl boron monoxide molecule (CH_3CCBO) plus the methyl radical. This data agrees very well with the reaction exoergicities extracted from NIST (-104 ± 5 kJ mol^{-1}) and also with our experimental data (-91 ± 22 kJ mol^{-1}).

Therefore, we can conclude that the 1-propynyl boron monoxide molecule (CH_3CCBO) presents the reaction product (R1/R3). A comparison of the molecular structures of the reactants and the final product suggests that one of the methyl groups of the dimethylacetylene reactant is replaced by the boron monoxide group. Considering that in the related reaction of boron monoxide with acetylene, the boron monoxide adds with its boron atom to the carbon–carbon triple bond forming a doublet radical intermediate (indirect scattering dynamics), we are proposing a similar reaction mechanism for the present system.[27] The reaction is expected to proceed *de facto via* the addition of the boron monoxide radical with its radical center located at the boron atom to the carbon–carbon triple bond of dimetylacetylene forming a doublet reaction intermediate which effectively undergoes unimolecular decomposition yielding the 1-propynyl boron monoxide molecule (CH_3CCBO) plus the methyl radical.

Our electronic structure calculations support these conclusions (Fig. 5–7). First, the boron monoxide radical and the dimethylacetylene reactant were found to react *via* addition of the boron monoxide radical with the radical center located at the boron atom to the carbon–carbon triple bonds yielding a *cis* (**i2**) and/or *trans* (**i3**) doublet radical intermediate; the *cis* structure can isomerize to its *trans* form (**i3**). Both **i2** and **i3** are connected *via* a transition state ranging only 20 kJ mol^{-1} above **i2**. Intermediate **i3** can undergo unimolecular decomposition *via* atomic hydrogen loss or methyl group elimination forming 1-methyl-propadienyl boron monoxide ($CH_3(BO)CCCH_2$; **p1**) or the 1-propynyl boron monoxide molecule (CH_3CCBO; **p3**). These reactions are overall exoergic by 29 kJ mol^{-1} and 105 kJ mol^{-1}, respectively, and involve tight exit transition states located 14 and 46 kJ mol^{-1} above the separated products. It should be mentioned that, several unsuccessful attempts were made to find a methyl loss pathway from intermediate **i2** to the 1-propynyl boron monoxide
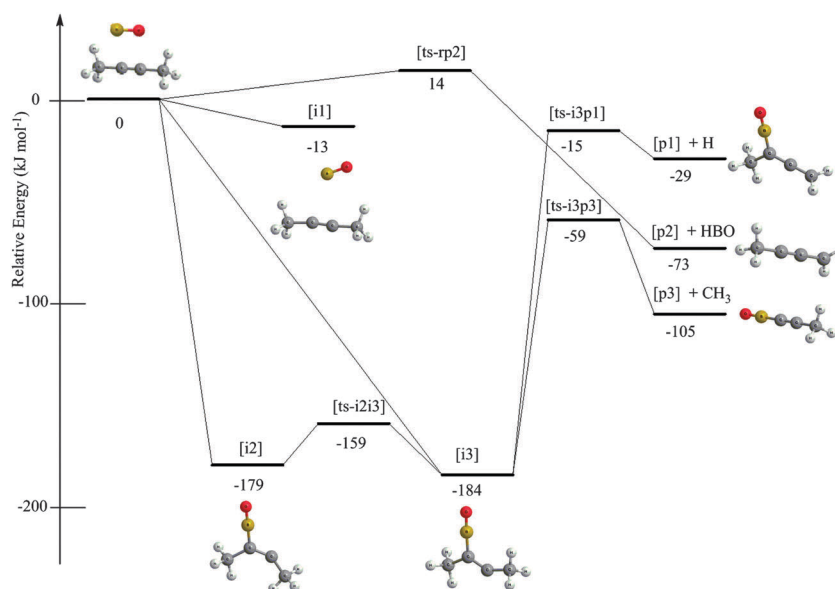

Fig. 5 Schematic representation of the computed $^{11}BOC_4H_6$ potential energy surface (PES).

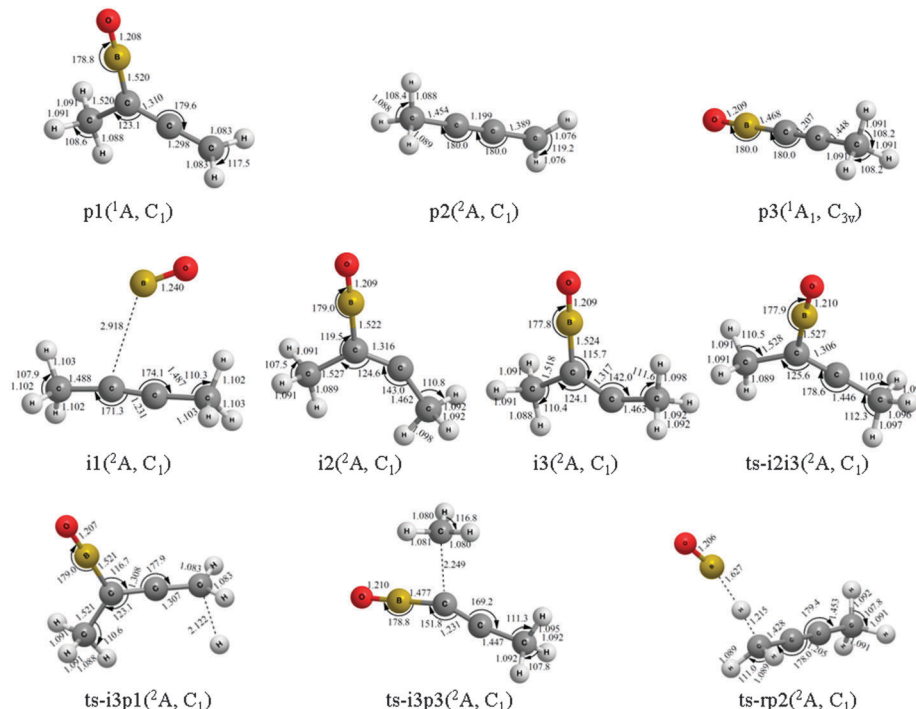**Fig. 6** Structures of reactants, intermediates, and products relevant to the $^{11}BOC_4H_6$ potential energy surface (PES). Bond lengths and angles are given in angstroms and degrees, respectively.

molecule (CH₃CCBO; **p3**). Recall that the indirect nature of the reaction *via* reaction intermediates has been predicted based on the shape of the center-of-mass angular distribution (R2). Further, the theoretically predicted tight exit transition state to form 1-the propynyl boron monoxide molecule (CH₃CCBO; **p3**) plus the methyl radical is also fully supported by our experiments predicting a tight exit barrier in the order of 20 to 40 kJ mol⁻¹ (R4). We would like to stress that intrinsic reaction coordinate calculations indicated the

Fig. 7 Typical intrinsic reaction coordinate (IRC) calculations of the entrance channel of the reaction of boron monoxide with dimethyl-acetylene leading to **i3**.

barrier-less nature of the addition of the boron monoxide radical (Fig. 7).

Our calculations also predict the existence of a weakly-bound van-der-Waals complex **i1** at the CCSD(T)/cc-pVTZ level of theory. It cannot be reproduced at the B3LYP/cc-pVTZ level. Optimization at B3LYP starting from **i1** collapses to **i2**. However, we are not successful in connecting the van-der-Waals complex **i1** to **i2** or **i3**. Therefore, if the van-der-Waals complex does exist, it would dissociate back to the reactants under single collision conditions.

It is important to comment on the non-detection and/or non-existence of the atomic hydrogen loss pathway forming 1-methyl-propadienyl boron monoxide (CH₃(BO)CCCH₂; **p1**). Both reaction products **p1** and **p3** originate from the unimolecular decomposition of the same reaction intermediate(s) **i2** and/or **i3**. The transition state(s) connection **i2** and/or **i3** with **p1** and **p3** are located 14 and 46 kJ mol⁻¹ below the energy of the separated reactants. This energy difference of 32 kJ mol⁻¹ together with the enhanced exoergicity of the **p3** *versus* **p1** channel (105 kJ mol⁻¹ and 29 kJ mol⁻¹) leads to an (almost) exclusive decomposition of intermediate **i3** *via* the lowest energy pathway to **p3**. These conclusions are also fully supported by our statistical (RRKM) calculations predicting a methyl group *versus* an atomic hydrogen loss branching ratio of 99.99% to 0.01% forming 1-propynyl boron monoxide (CH₃CC¹¹BO) and 1-methyl-propadienyl boron monoxide (CH₃(¹¹BO)CCCH₂), respectively. Note that the competing hydrogen abstraction channel yielding **p2** is likely to be less competitive considering the barrier of 14 kJ mol⁻¹ compared to the barrier-less addition to **i2**.

Finally, we would like to compare the results of the present study with the isoelectronic reaction of the cyano radical with
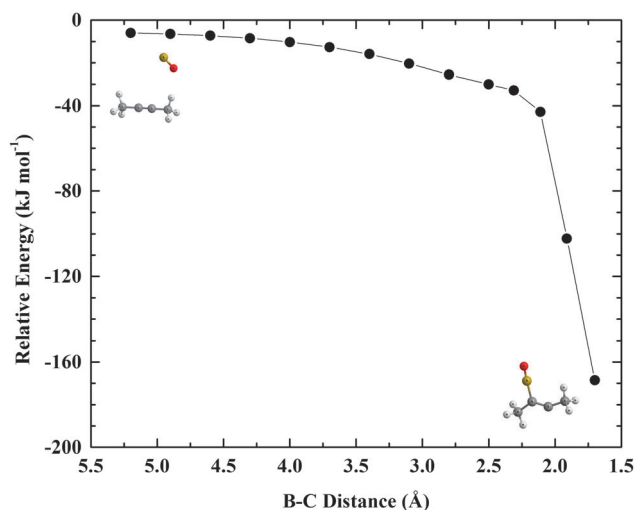
This journal is © the Owner Societies 2014

Phys. Chem. Chem. Phys., 2014, **16**, 989–997 | 995

dimethylacetylene studied under single collision conditions as well.[50] Here, the authors could identify the atomic hydrogen loss pathway leading to 1-methyl-propadienyl cyanide ($CH_3(CN)CCCH_2$) in an exoergic reaction (-70 kJ mol^{-1}). The competing methyl loss pathway forming 1-cyanomethylacetylene (CH_3CCCN; -123 kJ mol^{-1}) could not be monitored. Note that the authors generated the cyano radical *via* laser ablation of graphite and entraining the ablated products in nitrogen carrier gas, which also reacted as a reagent gas. The carbon co-reagent reacted with the dimethylacetylene molecule yielding a strong signal at $m/z = 65$ ($C_5H_5^+$), which had the same mass as the potential 1-cyanomethylacetylene (CH_3CCCN) product formed in the reaction of the cyano radical with dimethylacetylene. Since the concentration of atomic carbon was found to be a factor of about 50 larger than the cyano radical, reactive scattering of the cyano – dimethylacetylene forming 1-cyanomethylacetylene (CH_3CCCN) was likely masked by the signal at $m/z = 65$ ($C_5H_5^+$) from reaction of ground state carbon atoms with dimethylacetylene. Also, recall that the energy difference between the 1-methyl-propadienyl cyanide ($CH_3(CN)CCCH_2$) plus atomic hydrogen and 1-cyanomethylacetylene (CH_3CCCN) plus the methyl radical (cyano – dimethylacetylene) was only 53 kJ mol^{-1} compared to 76 kJ mol^{-1} for the 1-methyl-propadienyl boron monoxide ($CH_3(^{11}BO)CCCH_2$) plus atomic hydrogen and 1-propynyl boron monoxide ($CH_3CC^{11}BO$) plus methyl radical products (boron monoxide – dimethylacetylene). Considering similar heights of the exit barriers, the diminished energy difference in the competing exit channels of only 53 kJ mol^{-1} in the cyano – dimethylacetylene system compared to 76 kJ mol^{-1} for the boron monoxide – dimethylacetylene system can explain the experimental observation of the cyano *versus* atomic hydrogen loss pathway in the cyano – dimethylacetylene reaction, and the failed detection of the boron monoxide *versus* atomic hydrogen loss pathway in the boron monoxide – dimethylacetylene reaction. As a matter of fact, a recent *ab initio*/RRKM study on the cyano – dimethylacetylene system predicted branching ratios of the cyano *versus* atomic hydrogen loss channel of 1% compared to the 1-cyanomethylacetylene (CH_3CCCN) plus methyl radical channel (99%).[50]

6. Summary

We probed the crossed molecular beam reaction of boron monoxide (^{11}BO; $X^2\Sigma^+$) with dimethylacetylene (CH_3CCCH_3; X^1A_{1g}) at a collision energy of 23.9 ± 1.5 kJ mol^{-1} under single collision conditions. The scattering dynamics were found to be indirect *via* complex formation; the reaction started with an addition of the boron monoxide radical ($^{11}BO(X^2\Sigma^+)$) with the radical center located at the boron atom to the π electron density at the acetylenic carbon–carbon triple bond without an entrance barrier forming *cis–trans* $^{11}BOC_4H_6$ radical intermediates. *cis* $^{11}BOC_4H_6$ underwent *cis–trans* isomerization followed by unimolecular decomposition *via* a methyl group (CH_3) ejection to 1-propynyl boron monoxide ($CH_3CC^{11}BO$) in an overall exoergic reaction (experimental: -91 ± 22 kJ mol^{-1};

theoretical: -105 ± 9 kJ mol^{-1}; NIST: -104 ± 12 kJ mol^{-1}); *trans* $^{11}BOC_4H_6$ decomposed *via* a methyl group instantaneously. Both experiments and computations also predict a tight exit transition state suggesting that the reversed reaction, *i.e.* the addition of the methyl radical to the carbon–carbon triple bond of 1-propynyl boron monoxide ($CH_3CC^{11}BO$), holds a significant entrance barrier. The experimental finding of a sole methyl group loss gains full support from our computational study predicting fractions for the methyl group *versus* atomic hydrogen elimination of 99.99% to 0.01% forming 1-propynyl boron monoxide ($CH_3CC^{11}BO$) and 1-methyl-propadienyl boron monoxide ($CH_3(^{11}BO)CCCH_2$), respectively.

References

1 T. Edwards, *J. Propul. Power*, 2003, **19**, 1089–1107.
2 D.-X. Huo, G.-Q. He, L.-Q. Chen, N.-S. Liu and D.-Y. Ye, *Guti Huojian Jishu*, 2006, **29**, 329.
3 J. M. Mota, J. Abenojar, M. A. Martinez, F. Velasco and A. J. Criado, *J. Solid State Chem.*, 2004, **177**, 619–627.
4 S. H. Bauer, *Chem. Rev.*, 1996, **96**, 1907–1916.
5 R. C. Brown, C. E. Kolb, R. A. Yetter, F. L. Dryer and H. Rabitz, *Combust. Flame*, 1995, **101**, 221–238.
6 N. Balucani, F. Zhang and R. I. Kaiser, *Chem. Rev.*, 2010, **110**, 5107–5127.
7 M. K. King, *Combust. Sci. Technol.*, 1972, **5**, 155–164.
8 S. C. Li and F. A. Williams, *Symp. (Int.) Combust., [Proc.]*, 1991, **23**, 1147–1154.
9 C. L. Yeh and K. K. Kuo, *Prog. Energy Combust. Sci.*, 1996, **22**, 511–541.
10 W. Zhou, R. A. Yetter, F. L. Dryer, H. Rabitz, R. C. Brown and C. E. Kolb, *Combust. Flame*, 1999, **117**, 227–243.
11 B. Hussmann and M. Pfitzner, *Combust. Flame*, 2010, **157**, 822–833.
12 B. Hussmann and M. Pfitzner, *Combust. Flame*, 2010, **157**, 803–821.
13 S.-D. Li, J.-C. Guo and G.-M. Ren, *THEOCHEM*, 2007, **821**, 153–159.
14 C. Ollivier and P. Renaud, *Chem. Rev.*, 2001, **101**, 3415–3434.
15 A. Papakondylis and A. Mavridis, *J. Phys. Chem. A*, 2001, **105**, 7106–7110.
16 H.-J. Zhai, S.-D. Li and L.-S. Wang, *J. Am. Chem. Soc.*, 2007, **129**, 9254–9255.
17 N. Balucani, O. Asvany, A. H. H. Chang, S. H. Lin, Y. T. Lee, R. I. Kaiser, H. F. Bettinger, P. V. R. Schleyer and H. F. Schaefer III, *J. Chem. Phys.*, 1999, **111**, 7472–7479.
18 N. Balucani, O. Asvany, R. I. Kaiser and Y. Osamura, *J. Phys. Chem. A*, 2002, **106**, 4301–4311.
19 R. I. Kaiser and N. Balucani, *Acc. Chem. Res.*, 2001, **34**, 699–706.

996 | *Phys. Chem. Chem. Phys.*, 2014, **16**, 989–997

This journal is © the Owner Societies 2014

20 R. G. Macdonald and K. Liu, *J. Chem. Phys.*, 1990, **93**, 2431–2442.

21 P. Maksyutenko, F. Zhang, X. Gu and R. I. Kaiser, *Phys. Chem. Chem. Phys.*, 2011, **13**, 240–252.

22 F. Zhang, P. Maksyutenko and R. I. Kaiser, *Phys. Chem. Chem. Phys.*, 2012, **14**, 529–537.

23 M. Alagia, N. Balucani, P. Casavecchia, D. Stranges and G. G. Volpi, *J. Chem. Phys.*, 1993, **98**, 8341–8344.

24 B. R. Strazisar, C. Lin and H. F. Davis, *Science*, 2000, **290**, 958–961.

25 Note that singlet dicarbon is a closed shell species and not a radical.

26 M. F. Witinski, M. Ortiz-Suarez and H. F. Davis, *J. Chem. Phys.*, 2006, **124**, 094307–094312.

27 D. S. N. Parker, F. Zhang, P. Maksyutenko, R. I. Kaiser and A. H. H. Chang, *Phys. Chem. Chem. Phys.*, 2011, **13**, 8560–8570.

28 D. S. N. Parker, F. Zhang, P. Maksyutenko, R. I. Kaiser, S. H. Chen and A. H. H. Chang, *Phys. Chem. Chem. Phys.*, 2012, **14**, 11099–11106.

29 X. Gu, Y. Guo, F. Zhang, A. M. Mebel and R. I. Kaiser, *Faraday Discuss.*, 2006, **133**, 245–275.

30 X. Gu, Y. Guo and R. I. Kaiser, *Int. J. Mass Spectrom.*, 2005, **246**, 29–34.

31 X. B. Gu, Y. Guo, E. Kawamura and R. I. Kaiser, *Rev. Sci. Instrum.*, 2005, **76**, 083115.

32 Y. Guo, X. Gu and R. I. Kaiser, *Int. J. Mass Spectrom.*, 2006, **249–250**, 420–425.

33 Y. Guo, X. Gu, E. Kawamura and R. I. Kaiser, *Rev. Sci. Instrum.*, 2006, **77**, 034701.

34 X. Gu, Y. Guo, E. Kawamura and R. I. Kaiser, *J. Vac. Sci. Technol., A*, 2006, **24**, 505–511.

35 D. Proch and T. Trickl, *Rev. Sci. Instrum.*, 1989, **60**, 713–716.

36 P. Maksyutenko, D. S. N. Parker, F. Zhang and R. I. Kaiser, *Rev. Sci. Instrum.*, 2011, **82**, 083107.

37 X. Tan, *Diatomic*, CyberWit, Santa Clara, 1.4.1.1 edn, 2004.

38 M. Vernon, PhD thesis, University of California, Berkley, 1981.

39 M. S. Weis, PhD thesis, University of California, Berkley, 1986.

40 A. D. Becke, *J. Chem. Phys.*, 1993, **98**, 5648–5652.

41 C. Lee, W. Yang and R. G. Parr, *Phys. Rev. B: Condens. Matter*, 1988, **37**, 785–789.

42 M. J. O. Deegan and P. J. Knowles, *Chem. Phys. Lett.*, 1994, **227**, 321–326.

43 C. Hampel, K. A. Peterson and H. J. Werner, *Chem. Phys. Lett.*, 1992, **190**, 1–12.

44 P. J. Knowles, C. Hampel and H. J. Werner, *J. Chem. Phys.*, 1993, **99**, 5219–5227.

45 G. D. Purvis III and R. J. Bartlett, *J. Chem. Phys.*, 1982, **76**, 1910–1918.

46 M. J. Frisch, G. W. Trucks, H. B. Schlegel, G. E. Scuseria, M. A. Robb, J. R. Cheeseman, V. G. Zakrzewski, J. A. Montgomery, R. E. Stratmann, J. C. Burant, S. Dapprich, J. M. Millam, R. E. Daniels, K. N. Kudin, M. C. Strain, O. Farkas, J. Tomasi, V. Barone, M. Cossi, R. Cammi, B. Mennucci, C. Pomelli, C. Adamo, S. Clifford, J. Ochterski, G. A. Petersson, P. Y. Ayala, Q. Cui, K. Morokuma, P. Salvador, J. J. Dannenberg, D. K. Malick, A. D. Rabuck, K. Raghavachari, J. B. Foresman, J. Cioslowski, J. V. Ortiz, A. G. Baboul, B. B. Stefanov, G. Liu, A. Liashenko, P. Piskorz, I. Komaromi, R. Gomperts, R. L. Martin, D. J. Fox, T. Keith, M. A. Al-Laham, C. Y. Peng, A. Nanayakkara, M. Challacombe, P. M. W. Gill, B. Johnson, W. Chen, M. W. Wong, J. L. Andres, C. Gonzalez, M. Head-Gordon, E. S. Replogle and J. A. Pople, *GAUSSIAN 03, Revision C.02*, Gaussain, Inc., Wallingford, CT, 2004.

47 A. H. H. Chang, A. M. Mebel, X. M. Yang, S. H. Lin and Y. T. Lee, *J. Chem. Phys.*, 1998, **109**, 2748–2761.

48 R. I. Kaiser and A. M. Mebel, *Int. Rev. Phys. Chem.*, 2002, **21**, 307–356.

49 W. B. Miller, S. A. Safron and D. R. Herschbach, *Discuss. Faraday Soc.*, 1967, **44**, 108–122.

50 A. Jamal and A. M. Mebel, *J. Phys. Chem. A*, 2013, **117**, 741–755.

This journal is © the Owner Societies 2014

Phys. Chem. Chem. Phys., 2014, **16**, 989–997 | 997